RSC Advances

PAPER

View Article Online
View Journal | View Issue

Cite this: *RSC Adv.*, 2020, **10**, 12262

Cu/TEMPO catalyzed dehydrogenative 1,3-dipolar cycloaddition in the synthesis of spirooxindoles as potential antidiabetic agents†

Chitrala Teja,[a] Spoorthy N. Babu,[b] Ayesha Noor,[b] J. Arul Daniel,[c] S. Asha Devi[c] and Fazlur Rahman Nawaz Khan *[a]

Received 18th February 2020
Accepted 15th March 2020

DOI: 10.1039/d0ra01553a

rsc.li/rsc-advances

A series of spiro-[indoline-3,3′-pyrrolizin/pyrrolidin]-2-ones, **4**, **5** and **6** were synthesized in a sequential manner from Cu–TEMPO catalyzed dehydrogenation of alkylated ketones, **1** followed by 1,3-dipolar cycloaddition of azomethine ylides *via* decarboxylative condensation of isatin, **2** and L-proline/sarcosine, **3** in high regioselectivities and yields. The detailed mechanistic studies were performed to identify the reaction intermediates, which revealed that the reaction proceeds *via* dehydrogenative cycloaddition. Additionally, the regio and stereochemistry of the synthesized derivatives were affirmed by 2D NMR spectroscopic studies. The synthesized derivatives were explored further with molecular docking, *in vitro* antioxidant, and anti-diabetic activities.

1. Introduction

Spirooxindoles have recently attracted significant attention towards versatile bioactivities, such as antimicrobial,[1,2] anti-tumor,[3,4] anti-tubercular,[5,6] antiviral[7] and related properties.[8–12] Natural products, for instance, horsfiline, elacomine, alstonisine, mitraphylline,[13] spirotryprostatin A,[14,15] peteropodine, consist of a privileged heterocyclic skeleton, where the spiro ring is fused at the C3 position of the oxindole (Fig. 1).

The 1,3-dipolar cycloaddition[16–18] of azomethine ylides is the most efficient synthetic approach towards the spirooxindoles in high regio and stereoselectivities. Moreover, these spirooxindoles were generated by the decarboxylative condensation[19–21] of isatins and α-amino acids with unsaturated alkenes.[22–24] A wide variation of azomethine ylides,[25] including α-amino acids, and 1,3-dipolarophiles such as α,β-unsaturated carbonyl compounds,[26] (chalcones) arylidene-malono-dinitriles,[27] nitrostyrene,[28] acrylamides[29] α,β-unsaturated lactones,[30] and various electron-deficient alkenes have been extensively documented.

Fokas, Lalitha and co-workers utilized α,β-unsaturated carbonyl compounds and volatile toxic solvents, alike methanol and dioxane (Scheme 1).[23,31] Consequently, in the present study envisioned the α,β-unsaturated carbonyl intermediate, **1d** formation from Cu–TEMPO catalyzed dehydrogenation of the saturated ketone. TEMPO is a unique free radical (oxidant); was used as co-catalyst for several mechanistic studies.[32,33] In addition, several mechanistic pathways and reports were reported for dehydrogenation strategy. Nicolaou *et al.* developed a milder method using IBX (*o*-iodoxybenzoic acid) as a stoichiometric reagent,[34–36] Stahl *et al.*,[37–39] Newhouse *et al.*,[40] and others proposed aerobic dehydrogenation of alkyl aldehydes and ketones, using palladium, and other catalysis.[41–45] These reported methods were suffering from multistep reactions, expensive catalysts, and use of toxic volatile organic solvents (VOCs) Me–OH, Et–OH, 1,4-dioxane, toluene, DMF[46,47] and stoichiometric reagents, the formation of unwanted by-products and so forth.

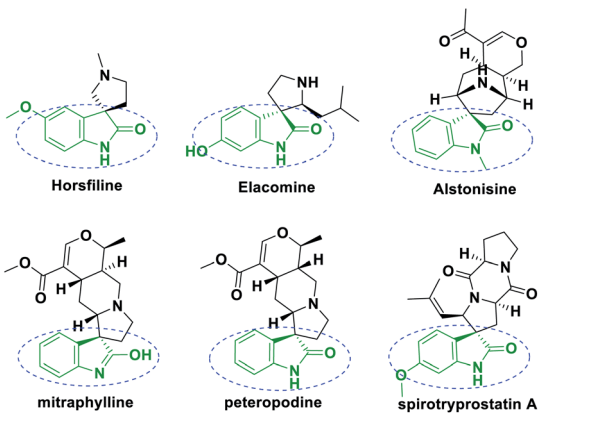

Fig. 1 Bioactive spirooxindole natural products.

[a]*Organic and Medicinal Chemistry Research Laboratory, Department of Chemistry, School of Advanced Sciences, Vellore Institute of Technology, Vellore-632014, Tamil Nadu, India. E-mail: nawaz_f@yahoo.co.in; Tel: +91-944-423-4609*

[b]*Centre for Bio Separation Technology, Vellore Institute of Technology, Vellore-632014, India*

[c]*Department of Biomedical Sciences, School of Bioscience and Technology, Vellore Institute of Technology, Vellore-632014, India*

† Electronic supplementary information (ESI) available: Copies of NMR, HRMS and FT-IR spectra of all compounds and 2D-NMR spectra for selected compounds. See DOI: 10.1039/d0ra01553a

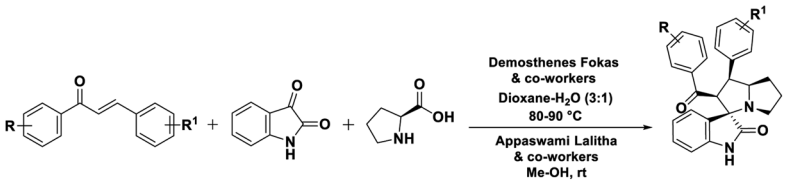

Scheme 1 1,3-Dipolar cycloaddition of α,β-unsaturated carbonyl compounds (previous work).

In order to overcome the above mentioned difficulties, herein, a Cu–TEMPO catalyzed dehydrogenative 1,3-dipolar cycloaddition of alkylated-ketones,[48] **1** utilizing isatin, **2**, and L-proline/sarcosine, **3**[48] in TBAA is reported for the spiro-indoline-3,3′-pyrrolizin/pyrrolidines (Scheme 2). Interestingly, the TBAA (tetrabutylammonium acetate) acted as a reaction medium instead of VOCs, in several C–C bond forming reactions.[46,47,49–54]

Likewise, diabetes mellitus (DM) type-2, a chronic metabolic disorder, was characterized by high blood sugar, insulin resistance, and secretion. The common symptoms were continual urination, increased hunger, and thirst, tiredness, and unexpected weight loss, and so forth.[55,56] According to the International Diabetes Federation (IDF) report as of 2017 approximately 425 million people were diagnosed with DM type 2.[57,58] There are numerous therapeutic approaches to treat diabetes, for instances, decreasing the postprandial hyperglycemia by hydrolyzing enzyme inhibition, including α-amylase and α-glucosidase.[59,60] Anti-diabetic inhibitors voglibose, Acarbose, and miglitol were utilized as drugs for years.[61–63] Lately, spirooxindoles were reported as anti-diabetic inhibitors,[64] therefore, the present work was envisioned to develop the spirooxindoles based anti-diabetic inhibitors.

2. Results and discussion

2.1 Chemistry

Initially, the reaction was carried out with 3-(4-fluorophenyl)-1-(*p*-tolyl)propan-1-one, **1ab** (0.5 mmol), and optimized the reaction conditions using transition metal catalysts *viz.* $Mn(OAc)_2$, $Co(OAc)_2$, $Ni(OAc)_2$, $Cu(OAc)_2$, $Zn(OAc)_2$, $Pd(OAc)_2$ (Table 1, entries 1–6) in the presence of TEMPO (0.1 mmol), 2,2-bipyridyl (0.1 mmol) in DMF at 100 °C. Interestingly, the $Cu(OAc)_2$ and $Pd(OAc)_2$ provided the desired unsaturated ketone **1d** within 4 h, through dehydrogenation of **1ab**. Further, the sequential addition of isatin (0.5 mmol) and L-proline (0.6 mmol) leads to the formation of spiro-oxindole **4ab** in 55% and 41% of yields, respectively. The TEMPO acted as a radical initiator, while the 2,2-bipyridyl as a bidentate transition metal chelating ligand for the reaction. Also, screened with Ag_2O, $CuSO_4$ $CuCl_2$, $CuBr_2$, and $Cu(OTf)_2$ under TEMPO/2,2-bipyridyl conditions, a trace amount of **4ab** was obtained (Table 1, entries 7–11). Likewise, the change of the ligand to 1,10-phenanthroline did not affect the yield of **4ab** (43% in 8 h) (Table 1, entry 12). Other tested ligands including, DBU, DABCO, and pyridine, respectively under the same experimental conditions, provided poor yields of **4ab** (Table 1, entries 13–15). Similarly, the change of the oxidant to *N*-hydroxyphthalimide (NHPI), *tert*-butyl-hydroperoxide (TBHP) using 2,2-bipyridyl in DMF at 100 °C provided a trace amount of **4ab** (Table 1, entries 16 and 17). In addition, screened the effect of solvent using 1,4-dioxane, DMSO, and toluene; however, there is no significant change in yield of the desired product was observed (Table 1, entries 18–20). Here all the optimizations were carried out sequentially by *in situ* addition of isatin and L-proline after the formation of unsaturated ketone intermediate from dehydrogenation of the saturated ketone.

Interestingly, when a sequential dehydrogenation/1,3-dipolar cycloaddition was screened using TBA-salt as a reaction medium instead of DMF by taking 3-(4-fluorophenyl)-1-(*p*-tolyl)propan-1-one **1ab** (0.5 mmol) TBAB (tetrabutylammonium-bromide) $Cu(OAc)_2$ (10%), TEMPO (0.1 mmol) and 2,2-bipyridyl (0.1 mmol) at 80 °C. It provided the corresponding spirooxindole **4ab** in good yield of 72% within 2 h (Table 1, entry 21). The TBAB acted as an ionic medium and was advantageous over VOCs, the TBA-salts also used in several C–C bond-forming transformations.[46,47,50,52,65–67] Encouraged by this result, further screened with various tetrabutylammonium-salts, for instances, TMAB (tetra-methylammonium bromide), TEAB (tetra-ethylammonium bromide), TBAA (tetra-butylammonium acetate), TBAI (tetra-butylammonium iodide) at 80 °C carried out, here **4ab** was obtained in good to excellent yields up to 87% (Table 1, entries 22–25). Among the tested TBA-salts, TBAA with 87% yield of desired product emerged out as the best-optimized condition (Table 1, entry 24). Additionally, when optimizing the loading of TBAA, for instance, 0.5 eq., 0.25 eq. (Table 1, entries 26 and 27) a less amount of product yield was observed while comparing with 1.0 eq.

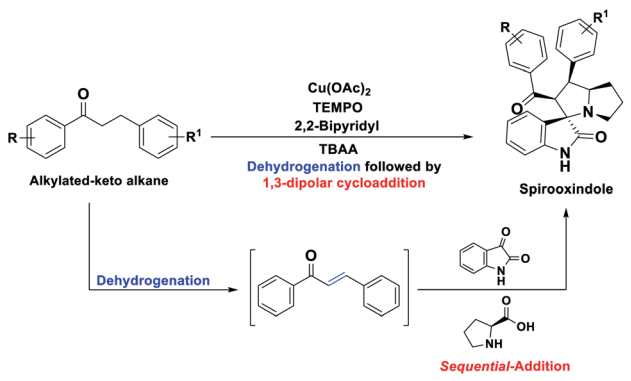

Scheme 2 Synthesis of spirooxindoles by sequential dehydrogenative 1,3-dipolar cycloaddition of alkylated ketones (this work).

Table 1 Optimization studies for preparation of spirooxindolopyrrolizidines[a,b,c]

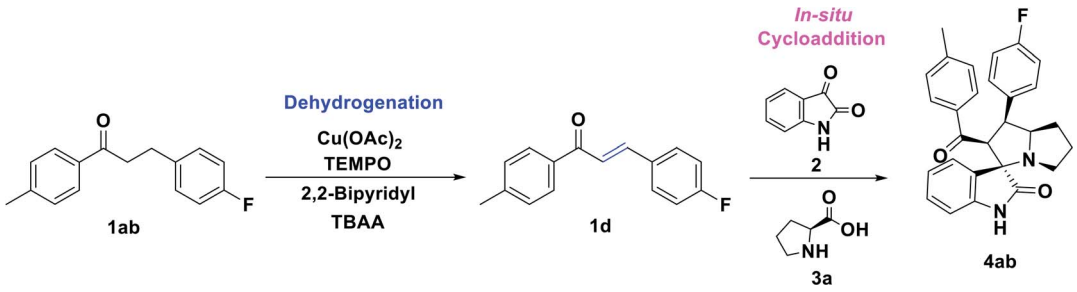

Entry	Cat. (mol%)	Additives		Solvent	Temp. °C	Time (h)	Yield% **4ab**[c]
1	$Mn(OAc)_2$	TEMPO	2,2′-Bipyridyl	DMF	100	9	—
2	$Co(OAc)_2$	TEMPO	2,2′-Bipyridyl	DMF	100	8	—
3	$Ni(OAc)_2$	TEMPO	2,2′-Bipyridyl	DMF	100	12	—
4	$Cu(OAc)_2$	TEMPO	2,2′-Bipyridyl	DMF	100	6	55
5	$Zn(OAc)_2$	TEMPO	2,2′-Bipyridyl	DMF	100	10	—
6	$Pd(OAc)_2$	TEMPO	2,2′-Bipyridyl	DMF	100	13	41
7	Ag_2O	TEMPO	2,2′-Bipyridyl	DMF	100	12	Trace
8	$CuSO_4$	TEMPO	2,2′-Bipyridyl	DMF	100	20	Trace
9	$CuCl_2$	TEMPO	2,2′-Bipyridyl	DMF	100	18	13
10	$CuBr_2$	TEMPO	2,2′-Bipyridyl	DMF	100	18	19
11	$Cu(OTf)_2$	TEMPO	2,2′-Bipyridyl	DMF	100	10	25
12	$Cu(OAc)_2$	TEMPO	1,10-Phenanthroline	DMF	100	8	43
13	$Cu(OAc)_2$	TEMPO	DBU	DMF	100	15	10
14	$Cu(OAc)_2$	TEMPO	DABCO	DMF	100	18	22
15	$Cu(OAc)_2$	TEMPO	Pyridine	DMF	100	12	15
16	$Cu(OAc)_2$	NHPI	2,2′-Bipyridyl	DMF	100	10	15
17	$Cu(OAc)_2$	TBHP	2,2′-Bipyridyl	DMF	100	15	15
18	$Cu(OAc)_2$	TEMPO	2,2′-Bipyridyl	1,4-Dioxane	100	10	31
19	$Cu(OAc)_2$	TEMPO	2,2′-Bipyridyl	DMSO	100	8	48
20	$Cu(OAc)_2$	TEMPO	2,2′-Bipyridyl	Toluene	100	16	25
21[b]	$Cu(OAc)_2$	TEMPO	2,2′-Bipyridyl	**TBAB (1 eq.)**	**80**	3	72
22	$Cu(OAc)_2$	TEMPO	2,2′-Bipyridyl	**TMAB**	**80**	4	63
23	$Cu(OAc)_2$	TEMPO	2,2′-Bipyridyl	**TEAB**	**80**	3	65
24	**$Cu(OAc)_2$**	**TEMPO**	**2,2′-Bipyridyl**	**TBAA**	**80**	2	**87**
25	$Cu(OAc)_2$	TEMPO	2,2′-Bipyridyl	**TBAI**	**80**	5	61
26	**$Cu(OAc)_2$**	**TEMPO**	**2,2′-Bipyridyl**	**TBAA (0.5 eq.)**	**80**	2	**82**
27	**$Cu(OAc)_2$**	**TEMPO**	**2,2′-Bipyridyl**	**TBAA (0.25 eq.)**	**80**	3	**70**

[a] Reaction conditions: saturated ketone, **1ab** (0.5 mmol), $Cu(OAc)_2$ (10 mol%), TEMPO (0.1 mmol) and 2,2-bipyridyl (0.1 mmol), in 2 mL of solvent at 100 °C after sequential addition of isatin, **2** (0.5 mmol), L-proline **3a** or sarcosine **3b** (0.6 mmol). [b] TBA-ionic-liquid (1 eq.) at 80 °C for 1 h. [c] Isolated yields.

Having streamlined optimized reaction condition in hand (Table 1, entry 24), various spirooxindole derivatives were obtained from different alkylated ketones by sequential dehydrogenative 1,3-cycloaddition, tabulated in Tables 2–4. Also, the scope of the reaction was explored using substrates with electron-donating groups (–Me, and –OMe), and with electron-withdrawing groups (–Cl, F and Br). Favorably, all the tested substrates transformed smoothly to provide the desired spirooxindoles.

2.2 Proposed reaction mechanism

In addition, the control experiments and ^{1}H NMR studies were performed to identify the reaction mechanism (results are discussed in Fig. S46 and 47 ESI Page S54–S56†). From the above mentioned mechanistic studies and previous literature reports,[45,68] we proposed the plausible reaction mechanism Fig. 2. Also, Su *et al.* previously proposed the plausible mechanistic pathway for dehydrogenation of saturated ketones *via* radical addition and elimination.[45]

Initially, $Cu(OAc)_2$ gets reacted with alkylated-ketone **A** to provide metal-enolate complex **B**. Then generates Cu(I) species, α-radical intermediate **C** and α-TEMPO radical substituted ketone **D**, as confirmed by ^{1}H NMR studies (ESI Fig. S47†).

Spectra-2 **C** reveals the α-TEMPO-adduct C–H proton at 4.6 ppm, where *trans*-ketone formation occurs, to form enones **E** and the formation of alkene (chalcone) *via* dehydrogenation **F**.

In (ESI Fig. S47†) **C** and **D** show the formation of unsaturated ketone (chalcone) along with saturated ketone. In the final step, oxidation occurs *via* Cu(I) species by TEMPO rather than

Table 2 Substrate scope with alkylated saturated ketones[a,b]

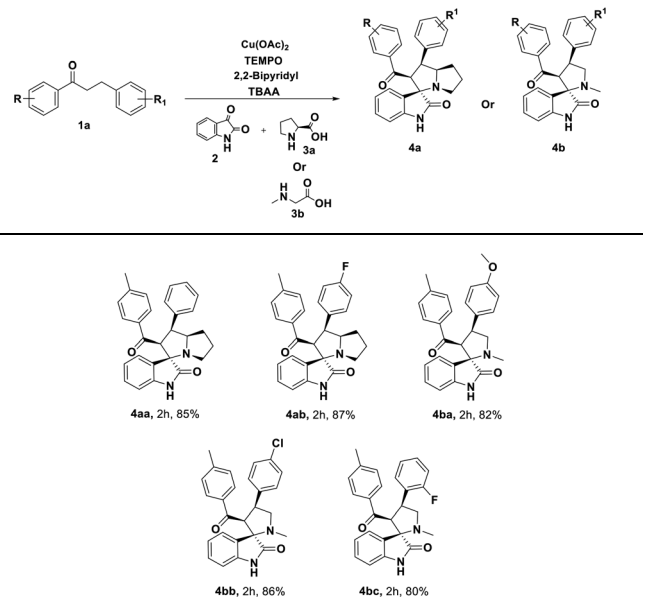

[a] Reaction conditions: alkylated ketone, **1a** (0.5 mmol), $Cu(OAc)_2$ (10 mol%), TEMPO (0.1 mmol) and 2,2′-bipyridyl (0.1 mmol), in TBAA (1 eq.) at 80 °C for 1 h, sequential addition of isatin, **2** (0.5 mmol), L-proline **3a** or sarcosine **3b** (0.6 mmol) at 80 °C for another 1 h. [b] Isolated yields.

Table 3 Substrate scope with quinolinyl-keto alkanes[a,b]

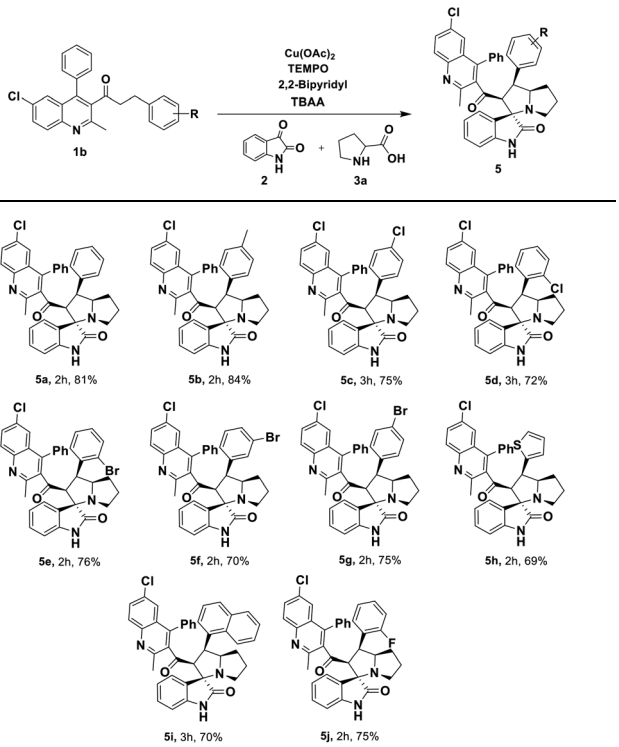

[a] Reaction conditions: quinolinyl-alkylated ketone, **1b** (0.5 mmol), $Cu(OAc)_2$ (10 mol%), TEMPO (0.1 mmol) and 2,2′-bipyridyl (0.1 mmol), in TBAA (1 eq.) at 80 °C for 1 h, sequential addition of isatin, **2** (0.5 mmol), L-proline **3a** or sarcosine **3b** (0.6 mmol) at 80 °C for another 1 h. [b] Isolated yields.

TEMPO-OH **G** to reproduce Cu(II) **H** by forming 2,2,6,6-tetramethylpiperidine and H_2O as by-products **I**.

The formation of Cu(II) species from the oxidation of Cu(I) species, was observed in literature reports.[69] The reactions of $Cu(OAc)_2$/2,2-bpy complex with TEMPO or TEMPO-OH have been demonstrated, the both TEMPO and TEMPO-OH could oxidize Cu(I) species to form Cu(II). Where the TBAA, as a basic and ionic medium, alters the reaction conditions. The sequential addition of isatin and proline to the unsaturated ketone intermediate (chalcone) resulted in the 1,3-dipolar cycloaddition leads to provide the 5-membered spirooxindoles. For instance, (Fig. 2) isatin **a**, L-proline **b** leads to carboxylative cyclic ester **c**, which undergoes decarboxylation **d** to give azomethine ylide **e**, a dipole. The azomethine ylide then undergoes 1,3-cycloaddition to provide the expected spirooxindole-1,3-dipolar-cycloaddition product **g**, water, and CO_2 only the by-products. The transformation of spirooxindole from unsaturated ketone has been indicated in (ESI Page S55, Fig. S47†) NMR studies. The structural elucidation of compounds **4**, **5**, and **6** were identified using ^1H, ^{13}C, and 2D-NMR spectroscopic studies (see ESI, Page S53†), as mentioned in the illustrative example of **4aa**.

2.3 Pharmacological studies

2.3.1 Molecular docking. The interaction study was carried out using AutoDock, and the results obtained are shown in Table 5. The interactions visualized using LigPlot+ are provided in (ESI Page S62–S66, Fig. S48–S50†) for interactions of the synthesized compounds with alpha-amylase, alpha-glucosidase, and GLP-1, respectively. The molecular docking study of the α-amylase enzyme with the synthesized compounds revealed the superior binding efficiency of the ligands when compared to the standard reference drug Acarbose. The commercial drug Acarbose had binding energy of −0.74 kcal mol^{-1}, and the synthesized compound **6c** and **6a** had the best binding energy of −9.61 and −9.51 kcal mol^{-1} respectively. Furthermore, the study revealed the interactions of the compounds with amino acid residues like TRP59, GLN63, ASP197, GLU233, ASP300 and HIS305 of the enzyme which is present in the active site of the enzyme and similar to the interaction with the standard drug Acarbose.[70]

Interaction of the synthesized compounds with α-glucosidase enzyme revealed that **6b** and **6a** had the best binding energy of −9.77 and −9.29 kcal mol^{-1}, respectively. Acarbose had binding energy of 0.32 kcal mol^{-1} and formed 3 hydrogen bonds with PHE525 and SER626 amino acid residues of the α-glucosidase enzyme. Most of the synthesized compounds had interactions with the catalytic domain of the α-glucosidase enzyme present between residues 358 to 720.[71] Molecular interactions with GLP-1 receptor revealed **6d**, **5a**, and **5b** had the best binding energy. Previous studies have shown that exendin-

Table 4 Substrate scope with quinolinyl-keto alkanes[a,b]

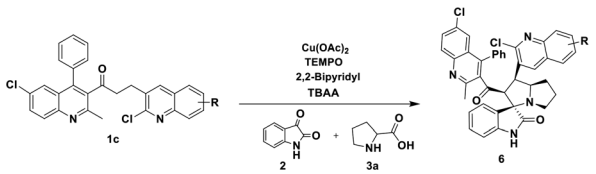

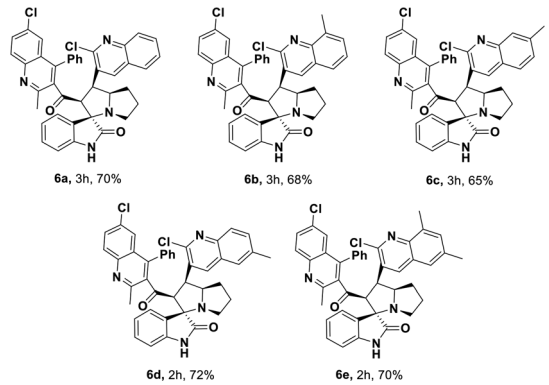

[a] Reaction conditions: quinolinyl-alkylated ketone, **1c** (0.5 mmol), $Cu(OAc)_2$ (10 mol%), TEMPO (0.1 mmol) and 2,2′-bipyridyl (0.1 mmol), in TBAA (1 eq.) at 80 °C for 1 hour, sequential addition of isatin, **2** (0.5 mmol), L-proline **3a** or sarcosine **3b** (0.6 mmol) at 80 °C for another 1 h. [b] Isolated yields.

Table 5 Binding energies of the synthesized molecules

S. no.	Compound name	Binding energy (kcal mol^{-1})		
		Alpha-amylase	Alpha-glucosidase	GLP-1
1	**5a**	−8.15	−8.64	−9.51
2	**5b**	−7.3	−8.08	−9.47
3	**5c**	−7.76	−8.66	−8.31
4	**5d**	−7.78	−8.27	−7.46
5	**5e**	−7.78	−7.6	−8.11
6	**5f**	−8.47	−7.23	−8.21
7	**5g**	−7.9	−7.61	−8.15
8	**5h**	−9.29	−7.28	−8.39
9	**5i**	−8.57	−8.73	−8.4
10	**5j**	−8.13	−7.91	−8.55
11	**6a**	−9.51	−9.29	−8.85
12	**6b**	−9.16	−9.77	−7.56
13	**6c**	−9.61	−7.07	−8.6
14	**6d**	−8.74	−7.44	−10.2
15	**6e**	−9.24	−8.71	−8.95
16	**4aa**	−7.81	−7.62	−7.65
17	**4ab**	−6.95	−7.04	−7.47
18	**4ba**	−6.77	−6.85	−6.66
19	**4bb**	−7.79	−7.14	−6.87
20	**4bc**	−7.78	−6.57	−7.31
21	Std. drug	−0.74	0.32	37.44

4 binds with the GLU128 of the GLP-1 receptor having an agonist activity (Underwood 2010).[72]

Current interaction studies have imparted that **5d**, **5f**, **5h**, **6e**, **4aa**, **4ab**, and **4bc** formed a hydrogen bond with GLU128, which implies that it could have agonist activity too as reported before.

2.3.2 *In vitro* antioxidant assay. All the synthesized compounds were tested for their anti-oxidant properties through various assays such as ABTS, DPPH, H_2O_2 scavenging assay, and metal chelating assay with the respective standards. All the compounds answered positively to these assays.

The reaction below shows the scavenging action of DPPH due to the presence of anti-oxidants

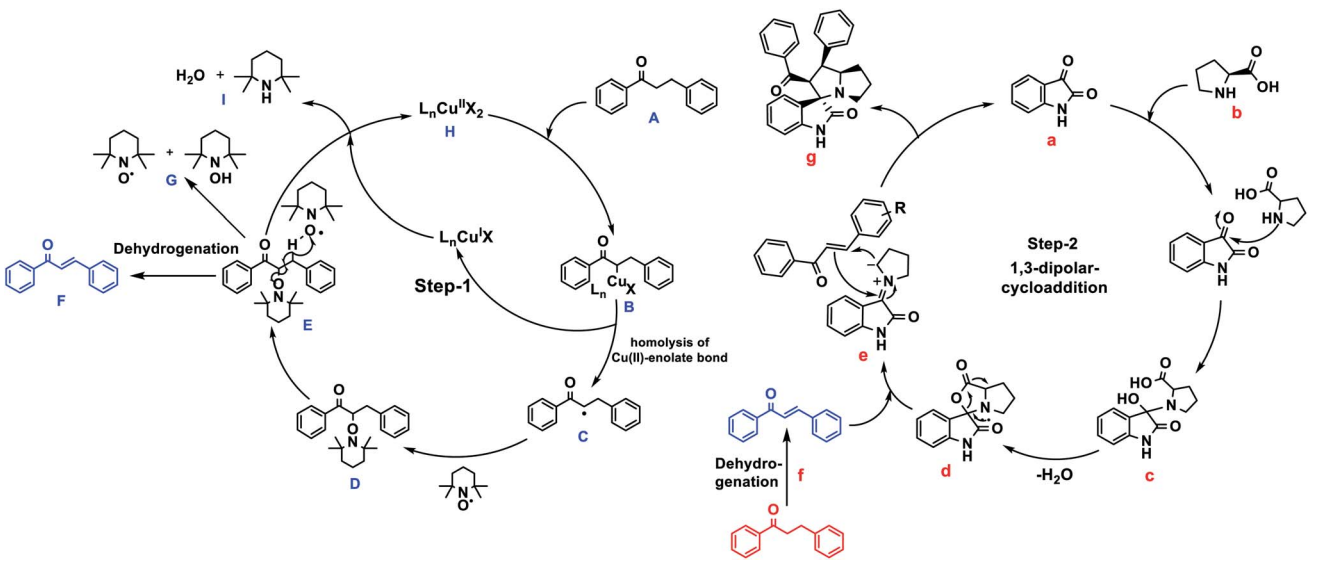

Fig. 2 Plausible mechanism for the synthesis of spirooxindoles from keto-alkanes *via* Cu–TEMPO catalyzed dehydrogenation and 1,3-dipolar cycloaddition.

All the synthesized compounds showed the potential to scavenge ABTS and DPPH radical with compound **6d** having the highest activity at an IC_{50} value of 0.28 ± 0.03 mg mL^{-1} and 0.34 ± 0.06 mg mL^{-1} respectively while compound **6e** had the least activity with an IC_{50} value of 6.04 ± 0.54 mg mL^{-1} and 6.98 ± 0.75 mg mL^{-1} respectively. The principle of metal chelating assay involves the chelation of ferrozine with ferrous ion. This forms a red-colored complex. The presence of antioxidants reduces the chelation as the antioxidants compete with ferrozine to chelate with the ferrous ion. The chelation of antioxidants with ferrous ion reduced the red color of the ferrozine ferrous ion complex.

In our study, all the compounds could chelate with ferrous ion. The compound **6e** exhibited highest potential (IC_{50} value: 0.31 ± 0.02 mg mL^{-1}) while compound **4ab** showed least potential with an IC_{50} value of 6.91 ± 1.10 mg mL^{-1}.

The H_2O_2 assay is based on the reduction of the tri-phenanthroline complex formed due to the reaction between ferrous ion and phenanthroline (red-orange). The addition of H_2O_2 reduced ferrous ion to ferric, and the tri-phenanthroline complex is not formed. The presence of compounds prevents the action of H_2O_2, leading to the formation of the tri-phenanthroline complex.

In our study, all compounds could scavenge the H_2O_2 radical with compound **5e** having the highest potential, while compound **4ab** had very less scavenging activity (shown in Table 6).

2.3.3 ***In vitro*** **anti-diabetic assay.** One of the factors for controlling diabetes is to reduce postprandial hyperglycemia. Inhibiting α-amylase and α-glucosidase enzymes reduced the postprandial hyperglycemia, and inhibitors of these enzymes are considered as potential antidiabetic agents, already discussed in the Introduction part.

In our study, all the compounds showed positive results in inhibiting the α-glucosidase enzyme with compounds **5h** and **5i** having high activity. It was interesting to note that only 7 compounds answered positively to the α-amylase inhibition assay with compounds **5h** and **5i** having higher potential.

Overall, amongst the compounds, it can be inferred that compounds **5h** and **5i** have anti-oxidant and anti-diabetic properties with better IC_{50} values (shown in Table 6).

2.3.4 QSAR-studies (quantitative structure–activity relationships)

2.3.4.1 Physicochemical and pharmacokinetic properties. The *in silico* physicochemical properties of synthesized spiro-oxindole analogs were calculated and compared with Acarbose (standard antidiabetic drug). All the compound molecular weights are calculated according to Lipinski's rule of 5, in that **4aa**, **4ab**, **4ba**, **4bb**, and **4bc**, which molecular weights are <500, remaining all the derivatives **5a** series and **6a** series including Acarbose are (>500) greater than its range. Polar Surface Area (PSA) is calculated based on TPSA methodology, TPSA is the essential factor that is showing molecular transport across the membranes, all the compounds showing TPSA values within satisfactory range between 50–100 except **4aa** series. So the result is showing our synthesized compounds showing moderate lipophilicity across the blood-brain barrier. Other parameters, like, number of rotatable bonds (*n*-RotB), number of O, N atoms present and NH, OH donor/acceptor, were also in acceptable range comparing with standard drug. The results are showing excellent properties comparing with Acarbose because electronic and steric, substitution factors of the molecules, the positive as well as negative results also were recorded. **4aa** series

Table 6 *In vitro* antioxidant and an anti-diabetic assay of the synthesized derivatives

S. no.	Compound	ABTS	DPPH	Metal chelating	H_2O_2	α-Amylase	α-Glucosidase
1	**4aa**	1.62 ± 0.21	1.46 ± 0.21	0.96 ± 0.23	0.63 ± 0.12	1.47 ± 0.27	1.48 ± 0.32
2	**4ab**	1.54 ± 0.30	1.22 ± 0.34	6.91 ± 1.10	6.15 ± 1.12	1.11 ± 0.41	1.52 ± 0.35
3	**4ba**	2.70 ± 0.60	1.23 ± 0.39	3.21 ± 0.76	0.88 ± 0.06	0.99 ± 0.06	1.25 ± 0.24
4	**4bb**	1.42 ± 0.31	0.80 ± 0.07	0.46 ± 0.08	0.41 ± 0.04	0.98 ± 0.25	1.46 ± 0.31
5	**4bc**	1.50 ± 0.45	1.68 ± 0.34	0.86 ± 0.09	1.16 ± 0.35	1.52 ± 0.40	2.22 ± 0.57
6	**5a**	3.25 ± 0.47	2.26 ± 0.13	0.93 ± 0.11	0.92 ± 0.09	NA	0.51 ± 0.19
7	**5b**	0.49 ± 0.32	0.55 ± 0.04	0.81 ± 0.06	0.79 ± 0.02	NA	2.73 ± 0.52
8	**5c**	1.57 ± 0.12	1.62 ± 0.43	0.92 ± 0.04	0.85 ± 0.07	NA	0.50 ± 0.03
9	**5d**	1.11 ± 0.36	1.28 ± 0.32	1.16 ± 0.31	1.50 ± 0.35	NA	1.02 ± 0.34
10	**5e**	0.79 ± 0.43	0.88 ± 0.09	6.00 ± 0.75	0.21 ± 0.03	NA	0.74 ± 0.13
11	**5f**	0.55 ± 0.20	0.50 ± 0.06	1.40 ± 0.62	1.52 ± 0.32	NA	0.30 ± 0.05
12	**5g**	2.72 ± 0.54	2.79 ± 0.32	0.69 ± 0.05	1.27 ± 0.32	NA	0.58 ± 0.06
13	**5h**	0.41 ± 0.06	0.49 ± 0.03	1.04 ± 0.08	0.78 ± 0.06	0.54 ± 0.14	0.35 ± 0.05
14	**5i**	0.86 ± 0.09	0.92 ± 0.05	0.77 ± 0.22	0.57 ± 0.09	0.28 ± 0.07	0.31 ± 0.07
15	**5j**	3.03 ± 0.65	2.09 ± 0.34	0.38 ± 0.07	0.35 ± 0.04	NA	1.12 ± 0.15
16	**6a**	2.75 ± 0.58	2.71 ± 0.43	0.43 ± 0.04	1.05 ± 0.27	NA	0.41 ± 0.04
17	**6b**	0.43 ± 0.05	0.44 ± 0.08	0.46 ± 0.08	0.68 ± 0.06	NA	0.26 ± 0.06
18	**6c**	0.34 ± 0.09	0.36 ± 0.02	0.99 ± 0.09	0.59 ± 0.03	NA	0.32 ± 0.07
19	**6d**	0.28 ± 0.03	0.34 ± 0.06	0.37 ± 0.03	0.33 ± 0.04	NA	0.24 ± 0.05
20	**6e**	6.04 ± 0.54	6.98 ± 0.75	0.31 ± 0.02	0.32 ± 0.07	NA	0.27 ± 0.02
21	Ascorbic acid	0.006 ± 0.002	NA	0.0073 ± 0.002	NA	NA	NA
22	Gallic acid	NA	0.0055 ± 0.001	NA	0.0045 ± 0.001	NA	NA
23	Acarbose	NA	NA	NA	NA	0.058 ± 0.012	0.046 ± 0.023

derivatives conceded 1 violation in terms of mlogPb violation, remaining all the compounds conceded 2 violations in terms of MW and mlogPb, comparing with Acarbose, which shows good results (Acarbose conceded 3 violations). So, according to Lipinski's rule of five, our compounds have no problems with bioavailability. In future new drug design and discovery point of view, a slight modification in the compounds may increase its lipophilicity and all other parameters (ESI Page S67, Table S7†).

The pharmacokinetics of the synthesized compounds were predicted using the pkCSM pharmacokinetic prediction tool to find the drug likeliness by ADMET properties (absorption, distribution, metabolism, excretion, and toxicity).[73]

The results show that all the synthesized molecules show excellent absorption properties including, water solubility, intestinal absorption, comparing with Acarbose as a standard drug. It shows moderate distribution properties and **4aa** series few derivatives show AMES toxicity, as well as hepatotoxicity; remaining derivatives do not have any toxicity issues. Based on the above results, all the synthesized molecules show excellent ADMET properties comparing with the standard drug (ESI Page S67, Table S8†).

3. Conclusions

In summary, we have developed a solvent-free protocol in the virtue of avoiding VOCs for the synthesis of novel spirooxindoles from alkylated saturated ketones *via* Cu–TEMPO catalyzed dehydrogenation and sequential 1,3-dipolar cycloaddition pathway. Also, the detailed mechanistic studies revealed that the reaction proceeds *via* dehydrogenation followed by cycloaddition. It is an efficient protocol in-terms of one-pot sequential strategy, in high regio, stereo-selectivities and yields. All the synthesized compounds were investigated further for bio-activities, such as *in silico* molecular docking, *in vitro* antioxidant and anti-diabetic activities, most of the synthesized derivatives shows potential anti-oxidant and anti-diabetic inhibition. QSAR-studies of the synthesized derivatives show good biodegradability and bioavailability, including drug transport and ADMET properties.

4. Experimental procedure

4.1 General information

All the chemicals were purchased from Sigma-Aldrich and TCI chemicals Ltd. used without further purification. All the reaction was conducted using glass reaction vials from App-tec Instrument Ltd., and performed by using in Apptec Lab Mate Manual Parallel Synthesizer. Pre-coated aluminum TLC sheets were used to check TLC (silica gel 60 F254, Merck). After completion of the reaction, the reaction mixture was allowed to warm at rt and extracted using water and CH_2Cl_2 as a solvent, and the organic extracts were dried over anhydrous Na_2SO_4, and the crude reaction mixture was passed through manual column chromatography to obtain pure product. Column chromatography performed on silica gel (100–200 mesh, Merck Ltd.) to give pure product on petroleum ether and ethyl acetate (petroleum ether/EtOAc 8 : 2 v/v). Characterization alike, NMR-spectra was recorded using Bruker AVANCE-III (400 MHz) using $CDCl_3$ as a solvent system. FT-IR spectra were recorded using (Shimadzu IR Tracer-100) spectrometer νmax are reported in cm^{-1}.

4.2 General procedure for synthesis of 1′-(4-fluorophenyl)-2′-(4-methylbenzoyl)-1′,2′,5′,6′,7′,7a′-hexahydrospiro[indoline-3,3′-pyrrolizin]-2-one (spirooxindole)

(3-(4-Fluorophenyl)-1-(*p*-tolyl)propan-1-one) saturated ketone, **1ab** (1.0 mmol), $Cu(OAc)_2$ (10 mol%), TEMPO (0.1 mmol) and 2,2-bipyridyl (0.1 mmol), in TBAA (1 eq.) at 80 °C for 1 h after formation of unsaturated enone intermediate **1d**, confirmed by TLC, sequential addition of isatin, **2** (0.5 mmol), L-proline **3a** or sarcosine **3b** (0.6 mmol) at 80 °C for another 1 h led to formation of 1′-(4-fluorophenyl)-2′-(4-methylbenzoyl)-1′,2′,5′,6′,7′,7a′-hexahydrospiro[indoline-3,3′-pyrrolizin]-2-one, as resulted spirooxindole, after confirmation of TLC, the reaction mixture was allowed to warm at rt and extracted using water and CH_2Cl_2 as solvent, and the organic extracts were dried over anhydrous Na_2SO_4, and the crude reaction mixture was passed through manual column chromatography to obtain pure product **4ab**.

The same procedure as follows for the synthesis of the remaining derivatives.

4.3 Molecular docking studies

Interaction studies were carried out for the synthesized derivatives with α-amylase, α-glucosidase, and glucagon-like peptide-1 (GLP-1). The structure of the compounds was obtained using ChemDraw, while the PDB structure of alpha-amylase, alpha-glucosidase, and GLP-1 were obtained from protein data bank with PDB ID 5U3A, 5NN8, and 3IOL respectively. AutoDock 4.2 was used to analyze the interactions, while LigPlot+ v1.4 was used to visualize the interactions. Interaction studies by AutoDock were carried out using different parameters for different targets. For alpha-amylase, the interacting grid points for *x*, *y*, and *z*-axis were set at 70, 80 and 70 of 0.9583 Å spacing, 90, 90, and 120 of 1.0 Å spacing for alpha-glucosidase and for GLP-1 it was set at 60, 90 and 80 at 0.7 Å spacing.

4.4 *In vitro* antioxidant assay

4.4.1 ABTS scavenging activity. ABTS assay was performed according to Rajurkar & Hande.[74] ABTS radical prepared was incubated with different concentrations of compounds in the dark for 15 minutes at 37 °C, and the absorbance was noted at 734 nm. The blank was run parallel in the same manner.

ABTS scavenging activity was calculated as follows:

$$\text{ABTS radical-scavenging activity (\%)} = [(A_c - A_s)/A_c] \times 100,$$

here A_c denotes the absorbance of the control reaction (containing all reagents except the sample), and A_s denotes the absorbance of the test sample.[74]

4.4.2 DPPH scavenging activity. The free radical scavenging activity at various concentrations (0.1, 0.25, 0.5, 1, 2 mg mL^{-1}) of compounds was evaluated by DPPH assay (Nikhat *et al.*, 2009).[75] The different concentrations of extract were vortexed with 1.0 mL of 0.1 mM of DPPH in methanol. The mixture was

incubated in the dark for 30 min at room temperature. The degree of inhibition of DPPH was monitored by a decrease in absorbance, which was measured at 517 nm against methanol solvent blank. The DPPH solution without extract served as control.[75] Scavenging activity was calculated as

$$\text{DPPH radical-scavenging activity (\%)} = [(A_c - A_s)/A_c] \times 100,$$

here A_c denotes the absorbance of the control reaction, and A_s denotes the absorbance of the test sample.

4.4.3 Hydrogen peroxide scavenging activity. H_2O_2 assay was performed by adding the test solution contained ferrous ammonium sulfate, 1,10-phenanthroline, hydrogen peroxide along with different concentrations of compounds tested for hydrogen peroxide scavenging activity and control solution contained only 1 mM ferrous ammonium sulfate and 1 mM 1,10-phenanthroline. Ascorbic acid used as a standard reference compound.[76] H_2O_2 scavenging activity was calculated as follows:

$$H_2O_2 \text{ radical-scavenging activity (\%)} = [(A_c - A_s)/A_c] \times 100,$$

where A_c denotes the absorbance of the control reaction, and A_s denotes the absorbance of the test sample.

4.4.4 Metal chelating assay. Metal chelating activity was measured by adding 0.1 mM ferrous sulfate (0.2 mL) and 0.25 mM ferrozine (0.4 mL) subsequently into different concentrations of compounds. After incubating at room temperature for 10 min, absorbance was recorded at 562 nm with ascorbic acid as a standard reference compound.[77] The metal chelating activity was calculated as follows:

$$\text{Metal chelating activity} = [(A_c - A_s)/A_c] \times 100,$$

where A_c denotes the absorbance of the control reaction, and A_s denotes the absorbance of the test sample.

4.5 α-Amylase inhibition assay

The α-amylase inhibition assay was performed using the 3,5-dinitrosalicylic acid (DNSA) method. The compounds were mixed with 0.25% starch azure and alpha-amylase (4 U mL^{-1}) solution. After 3 minutes, DNS was added and boiled for 15 minutes. The absorbance was noted at 540 nm. Acarbose was used as a standard reference compound. α-Amylase inhibition was calculated as follows:

$$\text{α-Amylase inhibition activity} = [(A_c - A_s)/A_c] \times 100,$$

where A_c denotes the absorbance of the control reaction, and A_s denotes the absorbance of sample.[69]

4.6 α-Glucosidase inhibition assay

α-Glucosidase inhibition of the compounds was measured with 1 mg mL^{-1} 4-nitrophenyl-α-D-glucopyranoside and α-glucosidase (0.3 U). After incubating at 37 °C for 30 min, the reaction was stopped by the addition of 50 mM sodium hydroxide, and the absorbance was recorded at 405 nm. Acarbose was used as the standard reference compound. α-Glucosidase inhibition was calculated as follows:

$$\text{α-Glucosidase inhibition activity} = [(A_c - A_s)/A_c] \times 100,$$

where A_c denotes the absorbance of the control reaction and A_s denotes the absorbance of the test sample.[69]

4.7 QSAR studies

Calculation of molecular physicochemical properties from Molinspiration online database server.

The pharmacokinetics of the synthesized compounds were predicted using the pkCSM pharmacokinetic prediction tool to find the drug likeliness by ADMET properties (absorption, distribution, metabolism, excretion, and toxicity).[73]

Conflicts of interest

The authors declare no competing financial interest.

Acknowledgements

The authors are thankful to SIF-VIT for providing NMR, GC-MS and IR and other instrumentation facilities.

Notes and references

1 I. Gülçin, M. Elmastaşan, A. Dandia, A. K. Jain and A. K. Laxkar, *RSC Adv.*, 2013, **3**, 8422–8430.
2 G. Periyasami, R. Raghunathan, G. Surendiran and N. Mathivanan, *Bioorg. Med. Chem. Lett.*, 2008, **18**, 2342–2345.
3 A. S. Girgis, *Eur. J. Med. Chem.*, 2009, **44**, 91–100.
4 B. Yu, D.-Q. Yu and H.-M. Liu, *Eur. J. Med. Chem.*, 2015, **97**, 673–698.
5 S. V. Karthikeyan, B. D. Bala, V. P. A. Raja, S. Perumal, P. Yogeeswari and D. Sriram, *Bioorg. Med. Chem. Lett.*, 2010, **20**, 350–353.
6 P. Prasanna, K. Balamurugan, S. Perumal, P. Yogeeswari and D. Sriram, *Eur. J. Med. Chem.*, 2010, **45**, 5653–5661.
7 T. Jiang, K. L. Kuhen, K. Wolff, H. Yin, K. Bieza, J. Caldwell, B. Bursulaya, T. Y.-H. Wu and Y. He, *Bioorg. Med. Chem. Lett.*, 2006, **16**, 2105–2108.
8 K. Ding, Y. Lu, Z. Nikolovska-Coleska, S. Qiu, Y. Ding, W. Gao, J. Stuckey, K. Krajewski, P. P. Roller and Y. Tomita, *J. Am. Chem. Soc.*, 2005, **127**, 10130–10131.
9 K. Ding, Y. Lu, Z. Nikolovska-Coleska, G. Wang, S. Qiu, S. Shangary, W. Gao, D. Qin, J. Stuckey and K. Krajewski, *J. Med. Chem.*, 2006, **49**, 3432–3435.
10 K. Lundahl, J. Schut, J. Schlatmann, G. Paerels and A. Peters, *J. Med. Chem.*, 1972, **15**, 129–132.
11 B. K. Yeung, B. Zou, M. Rottmann, S. B. Lakshminarayana, S. H. Ang, S. Y. Leong, J. Tan, J. Wong, S. Keller-Maerki and C. Fischli, *J. Med. Chem.*, 2010, **53**, 5155–5164.
12 G. Bhaskar, Y. Arun, C. Balachandran, C. Saikumar and P. T. Perumal, *Eur. J. Med. Chem.*, 2012, **51**, 79–91.

13 E. G. Prado, M. G. Gimenez, R. De la Puerta Vázquez, J. E. Sánchez and M. S. Rodriguez, *Phytomedicine*, 2007, **14**, 280–284.
14 C.-B. Cui, H. Kakeya and H. Osada, *Tetrahedron*, 1996, **52**, 12651–12666.
15 P. R. Sebahar and R. M. Williams, *J. Am. Chem. Soc.*, 2000, **122**, 5666–5667.
16 A. S. Babu and R. Raghunathan, *Tetrahedron*, 2007, **63**, 8010–8016.
17 K. V. Gothelf and K. A. Jørgensen, *Chem. Rev.*, 1998, **98**, 863–910.
18 W. S. Jen, J. J. Wiener and D. W. MacMillan, *J. Am. Chem. Soc.*, 2000, **122**, 9874–9875.
19 O. Tsuge, S. Kanemasa, M. Ohe and S. Takenaka, *Bull. Chem. Soc. Jpn.*, 1987, **60**, 4079–4089.
20 E. J. Corey, *J. Am. Chem. Soc.*, 1952, **74**, 5897–5905.
21 Y. Katsuyama, K.-i. Miyazono, M. Tanokura, Y. Ohnishi and S. Horinouchi, *J. Biol. Chem.*, 2011, **286**, 6659–6668.
22 J.-A. Xiao, H.-G. Zhang, S. Liang, J.-W. Ren, H. Yang and X.-Q. Chen, *J. Org. Chem.*, 2013, **78**, 11577–11583.
23 K. Revathy and A. Lalitha, *RSC Adv.*, 2014, **4**, 279–285.
24 S. Haddad, S. Boudriga, F. Porzio, A. Soldera, M. Askri, M. Knorr, Y. Rousselin, M. M. Kubicki, C. Golz and C. Strohmann, *J. Org. Chem.*, 2015, **80**, 9064–9075.
25 B. List, R. A. Lerner and C. F. Barbas, *J. Am. Chem. Soc.*, 2000, **122**, 2395–2396.
26 M. Yu, G. Li, S. Wang and L. Zhang, *Adv. Synth. Catal.*, 2007, **349**, 871–875.
27 A. Dandia, A. K. Jain and D. S. Bhati, *Tetrahedron Lett.*, 2011, **52**, 5333–5337.
28 N. Mase, R. Thayumanavan, F. Tanaka and C. F. Barbas, *Org. Lett.*, 2004, **6**, 2527–2530.
29 Y. H. Bae, T. Okano and S. W. Kim, *J. Polym. Sci., Part B: Polym. Phys.*, 1990, **28**, 923–936.
30 S. A. Glickman and A. C. Cope, *J. Am. Chem. Soc.*, 1945, **67**, 1017–1020.
31 D. Fokas, W. J. Ryan, D. S. Casebier and D. L. Coffen, *Tetrahedron Lett.*, 1998, **39**, 2235–2238.
32 L. Yu, H. Cao, X. Zhang, Y. Chen and L. Yu, *Sustainable Energy Fuels*, 2020, **4**, 730–736.
33 X. Deng, H. Cao, C. Chen, H. Zhou and L. Yu, *Sci. Bull.*, 2019, **64**, 1280–1284.
34 K. Nicolaou, Y.-L. Zhong and P. Baran, *J. Am. Chem. Soc.*, 2000, **122**, 7596–7597.
35 K. Nicolaou, T. Montagnon, P. Baran and Y.-L. Zhong, *J. Am. Chem. Soc.*, 2002, **124**, 2245–2258.
36 K. Nicolaou, T. Montagnon and P. S. Baran, *Angew. Chem., Int. Ed.*, 2002, **41**, 993–996.
37 T. Diao and S. S. Stahl, *J. Am. Chem. Soc.*, 2011, **133**, 14566–14569.
38 Y. Izawa, D. Pun and S. S. Stahl, *Science*, 2011, **333**, 209–213.
39 T. Diao, T. J. Wadzinski and S. S. Stahl, *Chem. Sci.*, 2012, **3**, 887–891.
40 Y. Chen, A. Turlik and T. R. Newhouse, *J. Am. Chem. Soc.*, 2016, **138**, 1166–1169.
41 M. Zhang, J. Zhou, J. Kan, M. Wang, W. Su and M. Hong, *Chem. Commun.*, 2010, **46**, 5455–5457.
42 W. Gao, Z. He, Y. Qian, J. Zhao and Y. Huang, *Chem. Sci.*, 2012, **3**, 883–886.
43 J. Zhou, G. Wu, M. Zhang, X. Jie and W. Su, *Chem.–Eur. J.*, 2012, **18**, 8032–8036.
44 Z. Wang, Z. He, L. Zhang and Y. Huang, *J. Am. Chem. Soc.*, 2018, **140**, 735–740.
45 X. Jie, Y. Shang, X. Zhang and W. Su, *J. Am. Chem. Soc.*, 2016, **138**, 5623–5633.
46 V. Calò, A. Nacci, A. Monopoli, A. Fornaro, L. Sabbatini, N. Cioffi and N. Ditaranto, *Organometallics*, 2004, **23**, 5154–5158.
47 V. Calo, A. Nacci, A. Monopoli, E. Ieva and N. Cioffi, *Org. Lett.*, 2005, **7**, 617–620.
48 C. Teja and F. R. Nawaz Khan, *ACS Omega*, 2019, **4**, 8046–8055.
49 V. Caló, A. Nacci, A. Monopoli, A. Detomaso and P. Iliade, *Organometallics*, 2003, **22**, 4193–4197.
50 H.-J. Xu, Y.-Q. Zhao and X.-F. Zhou, *J. Org. Chem.*, 2011, **76**, 8036–8041.
51 V. Calo, A. Nacci, A. Monopoli and F. Montingelli, *J. Org. Chem.*, 2005, **70**, 6040–6044.
52 A. M. Sajith and A. Muralidharan, *Tetrahedron Lett.*, 2012, **53**, 5206–5210.
53 J. M. Khurana and S. Kumar, *Tetrahedron Lett.*, 2009, **50**, 4125–4127.
54 A. Davoodnia, S. Allameh, A. Fakhari and N. Tavakoli-Hoseini, *Chin. Chem. Lett.*, 2010, **21**, 550–553.
55 D. Meetoo, P. McGovern and R. Safadi, *Br. J. Nurs.*, 2007, **16**, 1002–1007.
56 H. E. Lebovitz, *Clin. Chem.*, 1999, **45**, 1339–1345.
57 C. Almeida and R. Cruz, *Eur. J. Publ. Health*, 2019, **29**(suppl. 1), ckz034.088.
58 A. T. Kharroubi and H. M. Darwish, *World J. Diabetes*, 2015, **6**, 850.
59 G. Wang, Z. Peng, Z. Gong and Y. Li, *Bioorg. Chem.*, 2018, **78**, 195–200.
60 S. Shah, K. Javaid, H. Zafar, K. M. Khan, R. Khalil, Z. Ul-Haq, S. Perveen and M. I. Choudhary, *Bioorg. Chem.*, 2018, **78**, 269–279.
61 A. Chaudhury, C. Duvoor, R. Dendi, V. Sena, S. Kraleti, A. Chada, R. Ravilla, A. Marco, N. S. Shekhawat and M. T. Montales, *Front. Endocrinol.*, 2017, **8**, 6.
62 P. Guillausseau, *Diabetes Metabol.*, 2003, **29**, 79–81.
63 I. W. Campbell, *Drugs*, 2000, **60**, 1017–1028.
64 S. Mathusalini, T. Arasakumar, K. Lakshmi, C.-H. Lin, P. S. Mohan, M. G. Ramnath and R. Thirugnanasampandan, *New J. Chem.*, 2016, **40**, 5164–5169.
65 T. Jeffery and M. David, *Tetrahedron Lett.*, 1998, **39**, 5751–5754.
66 V. Calo, A. Nacci, A. Monopoli and A. Fanizzi, *Org. Lett.*, 2002, **4**, 2561–2563.
67 Y. Liu, M. Li, Y. Lu, G.-H. Gao, Q. Yang and M.-Y. He, *Catal. Commun.*, 2006, **7**, 985–989.
68 C. Teja and F. R. Nawaz Khan, *Org. Lett.*, 2020, **22**, 1726–1730.

69 A. Dijksman, I. W. Arends and R. A. Sheldon, *Org. Biomol. Chem.*, 2003, **1**, 3232–3237.
70 G. D. Brayer, G. Sidhu, R. Maurus, E. H. Rydberg, C. Braun, Y. Wang, N. T. Nguyen, C. M. Overall and S. G. Withers, *Biochemistry*, 2000, **39**, 4778–4791.
71 V. Roig-Zamboni, B. Cobucci-Ponzano, R. Iacono, M. C. Ferrara, S. Germany, Y. Bourne, G. Parenti, M. Moracci and G. Sulzenbacher, *Nat. Commun.*, 2017, **8**, 1111.
72 C. R. Underwood, P. Garibay, L. B. Knudsen, S. Hastrup, G. H. Peters, R. Rudolph and S. Reedtz-Runge, *J. Biol. Chem.*, 2010, **285**, 723–730.
73 D. E. Pires, T. L. Blundell and D. B. Ascher, *J. Med. Chem.*, 2015, **58**, 4066–4072.
74 N. S. Rajurkar and S. Hande, *Indian J. Pharmaceut. Sci.*, 2011, **73**, 146.
75 F. Nikhat, D. Satynarayana and E. Subhramanyam, *Asian J. Res. Chem.*, 2009, **2**, 218–221.
76 D. Mukhopadhyay, P. Dasgupta, D. S. Roy, S. Palchoudhuri, I. Chatterjee, S. Ali and S. G. Dastidar, *Free Radic. Antioxidants*, 2016, **6**, 124–132.
77 I. Gülçin, M. Elmastaş and H. Y. Aboul-Enein, *Phytother Res.*, 2007, **21**, 354–361.